Journal of Photonics for Energy

SPIEDigitalLibrary.org/jpe

Using admittance spectroscopy to quantify transport properties of P3HT thin films

Ka H. Chan
Shu K. So

SPIE

Using admittance spectroscopy to quantify transport properties of P3HT thin films

Ka H. Chan and Shu K. So
Hong Kong Baptist University, Department of Physics and Centre for Advanced Luminescence Materials, Kowloon Tong, Hong Kong, China
E-mail: skso@hkbu.edu.hk

Abstract. The charge transport properties of organic electronic materials are of critical importance for the understanding of the operation of organic photonic devices. We show in this study that admittance spectroscopy (AS), which is a measure of the frequency dependent capacitances of organic electronic materials, can be used to determine charge carrier mobilities and transport parameters in organic photovoltaic materials. A plot of the negative differential susceptance versus frequency yields a maximum at a frequency. The position of the maximum is related to the average carrier transit time. Using AS, we study the hole transport properties of thin films of poly(3-hexylthiophene) (P3HT) based materials for organic photovoltaic applications, including pristine P3HT, and P3HT doped with [6,6]-phenyl-C61-butyric acid methyl ester (PCBM). We demonstrate that AS can be used to extract hole mobilities of P3HT and P3HT:PCBM with a thickness of ∼350 nm. For P3HT:PCBM, copper phthalocyanine is used as an electron trapping layer to reduce the effect of negative capacitance. [DOI: 10.1117/1.3556727]

Keywords: charge transport; carrier mobility; admittance spectroscopy; P3HT, thin film; negative capacitance.

Paper 10112SSPR received Jul. 15, 2010; revised manuscript received Dec. 23, 2010; accepted for publication Jan. 31, 2011; published online Mar. 16, 2011.

1 Introduction

Conducting polymers have received a great deal of attention owing to their advantages, including flexibility, ease of fabrication, and low production cost. Organic light emitting diodes, organic thin film transistors (OTFTs), and organic photovoltaic (OPV) cells are the applications of those polymers.[1–3] OPV cell probably enjoys the most attractive application nowadays because it can convert solar energy into electricity. Nowadays, the power conversion efficiency (PCE) of polymer-based OPV cells has already reached ∼7 to 8%.[4,5] In order to further enhance the PCE, understanding of carrier transport mechanisms within the OPV cells is essential.

There exist different techniques to study carrier transport properties. Examples are time-of-flight (TOF), OTFT, dark-injection space-charge-limited current (DI-SCLC), charge extraction by linearly increasing voltage (CELIV), and admittance spectroscopy (AS).[6] However, not all the techniques are suitable for the organic thin film measurements. For TOF and DI-SCLC, there is a minimum requirement for the film thickness due to the penetration depth of incident laser and RC effect of the samples, respectively.[7] For OTFT, it can be used to determine the carrier mobilities in thin film (∼100 to 200 nm). However, the transport direction of the carriers is parallel to the substrate.[8] The extracted value may be different from OPV devices, in which the carriers transport in a direction perpendicular to the substrate. CELIV is a popular technique to measure the organic thin film in a perpendicular direction.[9] For CELIV to be useful, free carriers are required in the organic materials. Otherwise, an additional step is needed to generate the free carriers in samples.

1947-7988/2011/$25.00 © 2011 SPIE

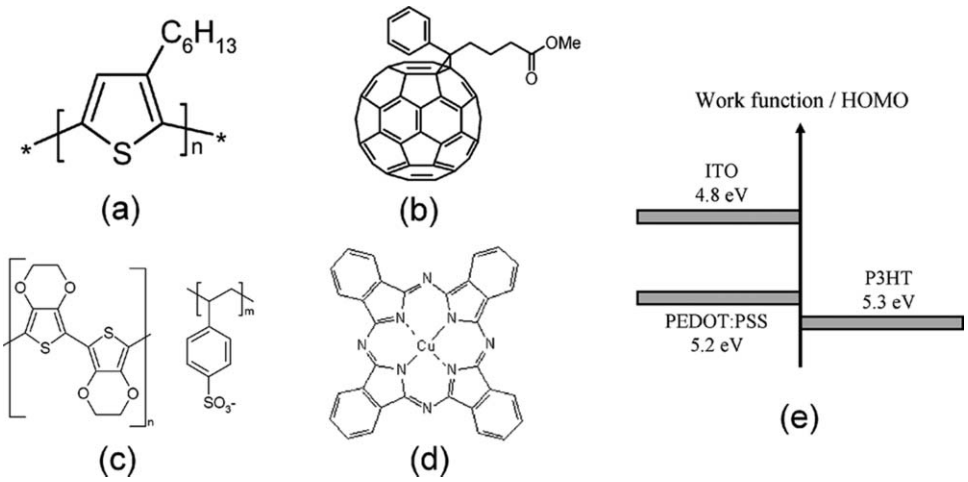

Fig. 1 Chemical structures of (a) P3HT, (b) PCBM, (c) PEDOT:PSS, and (d) CuPc. (e) Work functions of anodes and HOMO level of P3HT.

In this contribution, we show that AS is a viable technique to study carrier transport properties of organic thin films. The hole mobilities of poly(3-hexylthiophene) (P3HT) based materials, including pristine P3HT and P3HT:[6,6]-phenyl-C61-butyric acid methyl ester (PCBM), are investigated. In order to obtain ohmic contact, poly(3,4-ethylenedioxythioplene) doped with poly(strenesulfonate) (PEDOT:PSS) is inserted between the anode and the organic layer to reduce the hole injection barrier. In the study of P3HT:PCBM, copper phthalocyanine (CuPc) is inserted between the cathode and the organic layer and acts as an electron blocking layer to reduce the effect of negative capacitance. The chemical structures of different materials are shown in Figs. 1(a)–1(d), while the work functions of anodes and the highest occupied molecular orbital (HOMO) of P3HT are shown in Fig. 1(e).

2 Measurement Technique

AS is a very useful technique for determining carrier transport properties in organic semiconducting materials.[10–13] Generally, the device structure is anode/organic layer/cathode. To measure a reliable hole mobility, an ohmic contact is required between the anode and organic layer. In addition, there should be a large electron injection barrier by using a large work function cathode. If the sample is subjected to a dc biased voltage V_{dc} and a small ac signal υ_{ac} with frequency f, the frequency dependent admittance Y can be measured by an impedance analyzer. The admittance can be described by the following equation:

$$Y(\omega) = G + i\omega C, \tag{1}$$

where G is the conductance, C is the capacitance, and $\omega = 2\pi f$ is the angular frequency. Thus, the frequency dependent capacitance can be obtained from the imaginary part of the above expression. Figure 2(a) shows the typical features of C. At high frequencies, the capacitance remains constant and equals geometry capacitance C_{geo} because of the absence of ac charges through the sample. At intermediate frequencies, C starts to decrease due to the injected ac carriers. Those carriers that have a phase lag with the applied υ_{ac} result in an inductive contribution to C. At low frequencies, the measured capacitance increases again. The reason is that there is an additional capacitance with the trapping and releasing of charges from traps that are present in the organic material.

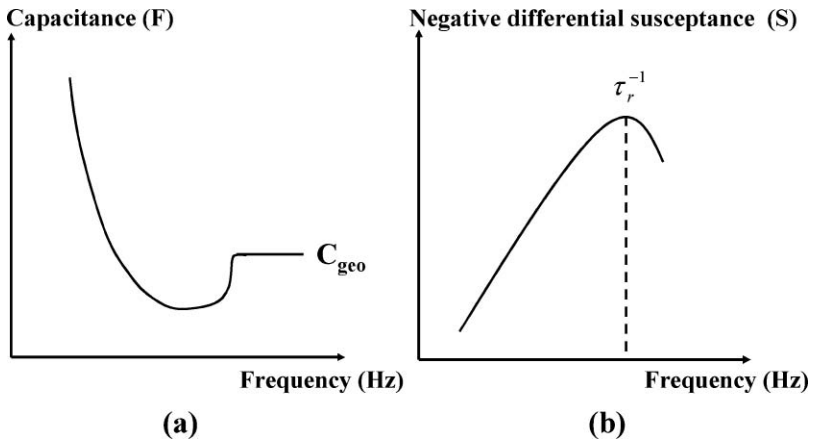

Fig. 2 (a) Typical frequency dependent capacitance signal. (b) Negative differential susceptance versus frequency plot.

In order to extract the hole mobilities, the negative differential susceptance $-\Delta B$ is first computed from the measured C using the following equation:

$$-\Delta B = -2\pi f(C - C_{\text{geo}}). \tag{2}$$

By plotting $-\Delta B$ versus f, the maximum point of $-\Delta B$ can be obtained at the frequency $f_r = \tau_r^{-1}$ as shown in Fig. 2(b). From a computer simulation, τ_r is correlated with the average transit time τ_{dc} by the relation $\tau_{\text{dc}} = 0.56\tau_r$.[11] With the known sample thickness d and the electric field F, the average carrier mobility can be calculated by:

$$\mu = \frac{d^2}{\tau_{\text{dc}} \cdot V} = \frac{d}{0.56\tau_r \cdot F}. \tag{3}$$

3 Experimental Details

In this study, P3HT was purchased from three different corporations, namely, Rieke Metals, Inc. (P200), Lum. Tech. (LT-S909), and Aldrich (445703). PCBM was obtained from Lum. Tech. (LT-S095). The PEDOT:PSS (Clevios P VP Al 4083) solution was obtained from H.C.

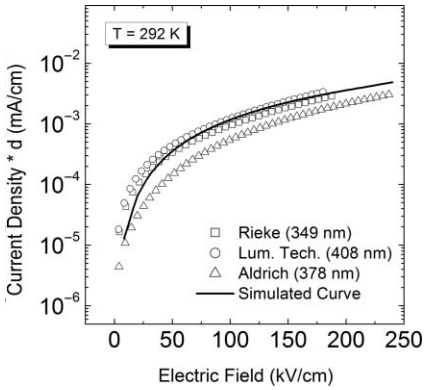

Fig. 3 J–V characteristics of different brands of P3HT films at $T = 292$ K. The solid line is the computed J_{SCL} with $\mu_0 = 7.59 \times 10^{-4}$ cm^2/Vs and $\beta = -2.33 \times 10^{-3}$ (V/cm)$^{-1/2}$ from Ref. 15.

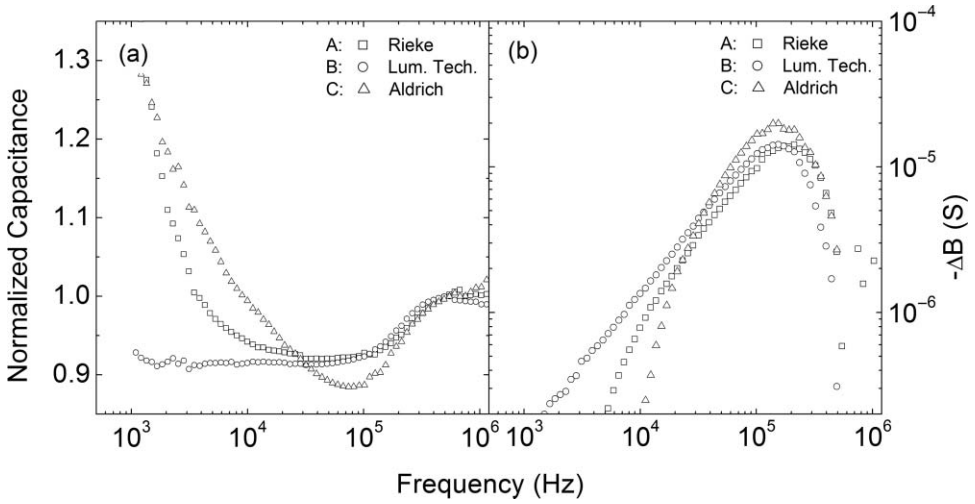

Fig. 4 (a) Frequency dependent capacitance and (b) negative differential susceptance plots of different brands of P3HT films at $T = 292$ K and $V_{dc} = 2$ V. The capacitance is normalized to the geometric capacitance.

Starks GmbH. The pre-patterned indium tin oxide (ITO) glass substrates were purchased from Tinwell Technology, Ltd., which were used as the bottom anode in the measurements. Before the deposition of organic layers, the ITO substrates were first cleaned by deconex. Then, deionized water and filtered acetone were used to rinse the substrates in an ultrasonic bath. Finally, the ITO substrates were exposed to UV-ozone for 13 min. in order to remove residual hydrocarbons on the surface.

For AS and *J–V* measurements, the structure of the device is ITO/PEDOT:PSS/P3HT or P3HT:PCBM/Au. The PEDOT:PSS solution was filtered by a 0.45-μm polyvinylidene fluoride (PVDF) filter and then it was spin-coated on the pretreated ITO for 90 s at 1000 rpm. The PEDOT:PSS layer was annealed at 150°C for 30 min in ambient in order to remove residual water. The film thickness of PEDOT:PSS was about 90 nm. Prior to the deposition of P3HT-based materials, it was first dissolved in 1,2-dichlorobenzene (DCB) with a concentration of 3 wt. % and stirred for 16 h at 40°C in dry nitrogen atmosphere inside a glove box. For the P3HT:PCBM blend, the raw materials were mixed in a ratio of 1:1 by weight and dissolved in DCB. The solutions were then spun on the top of the annealed PEDOT:PSS layer. The spinning speed and time

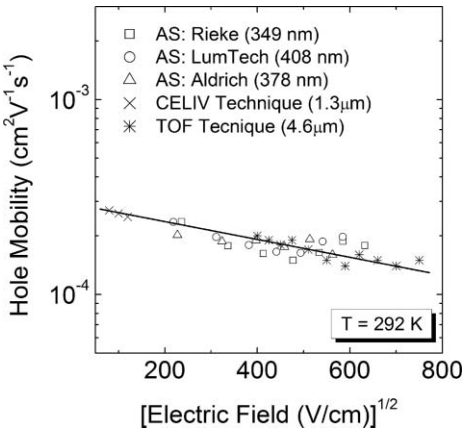

Fig. 5 Field dependent hole mobilities of different brands of P3HT films at $T = 292$ K. The star and cross symbols are the data obtained from TOF and CELIV from Refs. 16 and 17, respectively.

were 600 rpm and 30 s, respectively. Afterward, all the samples were dried naturally inside the glove box for 16 h under dark conditions. The resulting film thicknesses of P3HT-based materials were about 350 to 400 nm. After the spin-coating of organic layers, a gold electrode (the cathode) was coated on the polymer by thermal evaporation under a base pressure of $10^{\#x2212;6}$ Torr. The thickness of an Au electrode was 100 nm. The coating rate of Au was kept at 0.5 nm/s. In some P3HT:PCBM devices, 10 nm of CuPc was deposited on top of the P3HT:PCBM layer before cathode fabrication. After all the fabrications, the measurements were performed in vacuum ($\sim 10^{-3}$ Torr) inside a liquid nitrogen cooled cryostat (Oxford Instrument, Model ITC 601). In AS measurement, the admittances of the devices were measured by an impedance analyzer (Hioki E. E. Corp., Model 3532–50 LCR HiTESTER) as a function of frequency ($f = 10^3 - 5 \times 10^6$ Hz). A fixed ac modulation at 50 mV was superimposed on the dc bias voltage (0 to 10 V) during measurements. For the current-voltage (J–V) measurement, the samples were connected to the source-measure-unit (SMU) (Keithley Instruments Inc., Model 236). The signal (corresponding current) was then captured by driving a voltage to the sample from the SMU.

4 Results and Discussion

4.1 *Evaluation of Hole Transport Properties of Different Brands of P3HT*

Figure 3 shows the experimental J–V characteristics of different brands of P3HT films. The thicknesses are in the range of 349 to 408 nm. The solid line is the simulated SCLC (J_{SCL}) curve, which is computed by:[14]

$$J_{\mathrm{SCL}} = \frac{9}{8}\mu_0\varepsilon_0\varepsilon_r \exp(0.89\beta\sqrt{F})\frac{F^2}{d}, \tag{4}$$

where μ_0 is the zero-field mobility, β is the Poole–Frankel slope, ε_0 is the permittivity in vacuum, and $\varepsilon_r \approx 3$ is the dielectric constant. $\mu_0 = 7.59 \times 10^{-4}$ cm^2/Vs and $\beta = -2.33 \times 10^{-3}$ (V/cm)$^{-1/2}$ were obtained from TOF experiments.[15] It represents the theoretically maximum current that can be present in the film. For the P3HT obtained from Rieke and Lum. Tech., there are excellent agreements between the data and the theoretical J_{SCL}. The J–V data for P3HT from Aldrich are slightly lower than the ideal J_{SCL}. However, the departure from the J_{SCL} is well within half an order, especially at high voltages. It is conceivable that shallow traps are present for this batch of P3HT. Additional evidence from AS will be provided below.

For ease of discussion below, we label the different brands of P3HT by Brands A, B, and C that correspond to P3HT from Ricke, Lum. Tech., and Aldrich, respectively. Figure 4(a) shows the frequency dependent capacitances at $T = 292$ K and $V_{\mathrm{dc}} = 2$ V, normalized to the geometric capacitance C_{geo}. At high frequency (400 kHz), a clear C_{geo} can be clearly observed for all samples. As the probing frequency is reduced, the capacitance decreases. For samples A and B, the capacitances remain nearly constant between 10^4 to 10^5 Hz. In contrast, for sample C, the capacitance in the same range of frequencies reaches a minimum at about 90 kHz, and increases again. From Sec. 2, we conclude that carrier trapping and dispersion are more severe in sample C, when compared to samples A and B. This conclusion is also supported by the J–V data in Fig. 3. Due to the trapping effect, the capacitance increases again at low frequency.

Figure 4(b) shows the negative differential susceptance $-\Delta B$ versus frequency plot. The average transit time τ_{dc} can be obtained from the peak of the plot. As a result, the average hole mobilities can be calculated by Eq. (3). Figure 5 shows the extracted hole mobilities at different applied voltages at $T = 292$ K and the trends of the mobilities are in agreement with the Poole–Frenkel relation $\mu \propto \exp(\beta F^{1/2})$. The extracted mobilities are in good agreement with the data obtained independently from TOF and CELIV techniques (as shown in Fig. 5), in which much thicker films are used for measurements.[16,17] The excellent agreement among the data sets establishes the reliability of the AS technique for the transport characterization of

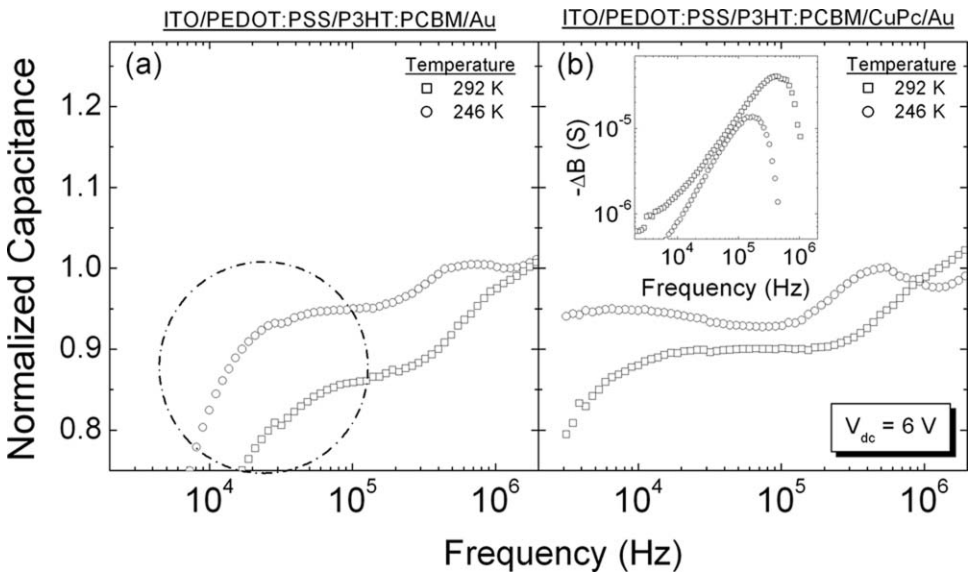

Fig. 6 Frequency dependent capacitance of P3HT:PCBM films at different temperatures and $V_{dc} = 6$ V (a) without. CuPc layer and (b) with a CuPc layer. In (a), the dotted circle indicates the low frequency regime in which negative contribution to the capacitance occurs. In (b), the inset shows the negative differential susceptance plots of P3HT:PCBM films with a CuPc layer.

P3HT films. However, the average hole mobilities of P3HT are found to exhibit a negative field dependence. This phenomenon is widely observed in the P3HT transport measurements.[16,17] The origin(s) of this phenomenon is still under debate. One proposed explanation is that the positional disorder of materials is larger than its energetic disorder.[18] Recently, it was observed that P3HT can form nanorods.[19] It is conceivable that these nanorods may influence the low field transport by opening up alternative pathways. These pathways are not necessarily along the direction of the applied field and therefore, carrier mobility may decrease as the applied field increases.

4.2 *Evaluation of Hole Transport Properties of P3HT:PCBM*

Apart from the pristine P3HT, the charge carrier transport properties of P3HT:PCBM are also investigated by AS. The structure of the sample is ITO/PEDOT:PSS/P3HT:PCBM/Au. In this experiment, we chose P3HT from Rieke Metals, Inc. as it provides a better agreement between the experimental data and theoretical simulation for both J–V and AS measurements. Furthermore, P3HT from Rieke appears to be the most popular material provider for OPV fabrication from the literature.[20] The frequency dependent capacitances of P3HT:PCBM film at $T = 246$ K and $T = 292$ K are shown in Fig. 6(a). The data appear to be markedly different from the case of pure P3HT films. Between 10^5 to 10^6 Hz, the data are similar to the case of P3HT. However, there is a rapid reduction of capacitance in lower frequencies. One proposed explanation is that there is minority carrier injection during the measurement.[21–23] In this case, electrons are injected from the cathode and transport via the PCBM domains within the device. Thus, the active layer contains both holes and electrons. At the P3HT/PCBM interface, recombination occurs, resulting in the recombination current. This current generally lags behind the stimulus. As a result, there is a negative contribution to the frequency dependent capacitance. With the presence of the negative capacitance, it is difficult to determine the reliable value of the hole mobility.

In order to suppress this effect, a material with a low electron mobility is inserted between the cathode and P3HT:PCBM layer to impede the injected electrons. In this study, CuPc is

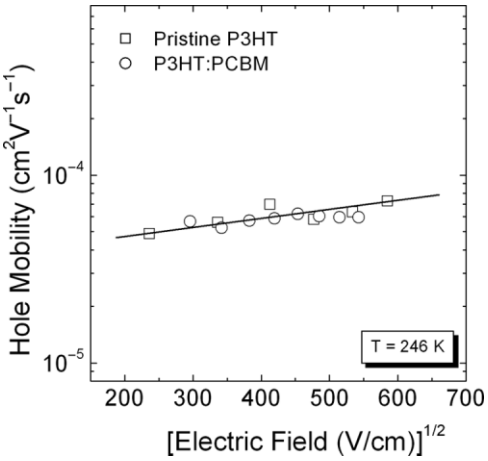

Fig. 7 Field dependent hole mobilities of P3HT:PCBM films at $T = 246$ K with the CuPc electron blocking layer. For comparison, the hole mobilities of P3HT (Rieke) is also shown.

chosen since it exhibits electron trapping behavior after air exposure. Figure 6(b) shows the frequency dependent capacitances at $T = 246$ K with the presence of a CuPc layer. It can be clearly observed that the effect of negative capacitance is effectively contained. The extracted hole mobilities of P3HT:PCBM are shown in Fig. 7. The mobility of the P3HT:PCBM blend is similar to the case of pristine P3HT. This result indicates that the percolation pathways of P3HT are unaffected by the presence of PCBM domains. Similar results were obtained previously from time-of-flight techniques in which much thicker films were used.[24]

In addition to $T = 246$ K, we also show in Fig. 6(b) data at $T = 292$ K. In contrast to the former case ($T = 246$ K), we still observe a decrease (less severe) of the capacitance at low frequencies. In this case, with a higher temperature, it is likely that there is still non-negligible injection of electrons, contributing to the addition reduction of capacitance. The CuPc layer probably is not the most effective electron blocking material. Materials with either a high-lying LUMO or electron blocking capabilities will be tested to improve the AS signal.

5 Conclusion

In conclusion, we have demonstrated that AS is a reliable technique to investigate the carrier transport properties of P3HT-based materials in a thin film (350 to 400 nm). For the pristine P3HT, the extracted hole mobilities are in good agreement with the data determined independently by TOF and CELIV techniques. For P3HT:PCBM, negative capacitance occurs at a low frequency due to the injection of electrons from the cathode. This phenomenon can be circumvented by inserting an electron blocking layer (CuPc). Thus, hole mobility can be determined reliably in a blend of P3HT:PCBM.

Acknowledgments

Support of this research by the Research Grant Council of Hong Kong under Grant No. HKBU210608E is gratefully acknowledged.

References

1. J. H. Burroughes, D. D. C. Bradley, A. R. Brown, R. N. Marks, K. Mackay, R. H. Friend, P. L. Burns, and A. B. Holmes, "Light-emitting diodes based on conjugated polymers," *Nature (London)* **347**, 539–541 (1990).

2. Y. Q. Liu and Y. G. Wen, "Recent progress in n-channel organic thin-film transistors," *Adv. Mater.* **22**, 1331–1345 (2010).
3. W. Cai, X. Gong, and Y. Cao, "Polymer solar cells: Recent development and possible routes for improvement in the performance," *Sol. Energy Mater. Sol. Cells* **94**, 114–127 (2010).
4. Y. Liang, Z. Xu, J. Xia, S. T. Tsai, Y. Wu, G. Li, C. Ray, and L. Yu, "For the bright future–Bulk heterojunction polymer solar cells with power conversion efficiency of 7.4%," *Adv. Mater.* **22**, E135–E138 (2010).
5. H. Y. Chen, J. Hou, S. Zhang, Y. Liang, G. Yang, Y. Yang, L. Yu, Y. Wu, and G. Li, "Polymer solar cells with enhanced open-circuit voltage and efficiency," *Nat. Photon.* **3**, 649–653 (2009).
6. S. K. So, S. C. Tse, and C. H. Cheung, *Organic Electronics: Materials, Processing, Devices and Applications*, F. So, Ed., Chap. 3, CRC Press, Francis and Taylor, Kowloon Tong, Hong Kong, China (2010).
7. J. Y. Song, N. Stingelin, W. P. Gillin, and T. Kreouzis, "Reduced hole mobility due to the presence of excited states in poly-(3-hexylthiophene)" *Appl. Phys. Lett.* **93**, 233306 (2008).
8. C. H. Cheung, K. K. Tsung, K. C. Kwok, and S. K. So, "Using thin film transistors to quantify carrier transport properties of amorphous organic semiconductors," *Appl. Phys. Lett.* **93**, 083307 (2008).
9. G. Juška, K. Genevičius, K. Arlauskas, R. Österbacka, and H. Stubb, "Charge transport at low electric fields in π-conjugated polymers," *Phys. Rev. B* **65**, 233208 (2002).
10. H. C. F. Martens, H. B. Brom, and P. W. M. Blom, "Frequency-dependent electrical response of holes in poly(*p*-phenylene vinylene)," *Phys. Rev. B* **60**, R8489–R8492 (1999).
11. S. W. Tsang, S. K. So, and J. B. Xu, "Application of admittance spectroscopy to evaluate carrier mobility in organic charge transport materials," *J. Appl. Phys.* **99**, 013706 (2006).
12. S. W. Tsang, S. C. Tse, K. L. Tong, and S. K. So, "PEDOT:PSS polymeric conducting anode for admittance spectroscopy," *Org. Electron.* **7**, 474–479 (2006).
13. K. K. Tsung and S. K. So, "Advantages of admittance spectroscopy over time-of-flight technique for studying dispersive charge transport in an organic semiconductor," *J. Appl. Phys.* **106**, 083710 (2009).
14. P. N. Murgatroyd, "Theory of space-charge-limited current enhanced by Frenkel effect," *J. Phys. D: Appl. Phys.* **3**, 151–156 (1970).
15. K. Yang, Y. Wang, A. Jain, L. Samulson, and J. Kumar, "Determination of electron and hole mobility of regioregular poly(3-hexylthiophene) by the time of flight method," *J. Marco. Sci. A: Pure Appl. Chem.* **44**, 1261–1264 (2007).
16. A. J. Mozer and N. S. Sariciftci, "Negative electric field dependence of charge carrier drift mobility in conjugated, semiconducting polymers," *Chem. Phys. Lett.* **389**, 438–442 (2004).
17. A. J. Mozer, N. S. Sariciftci, A. Pivrikas, R. Österbacka, G. Juška, L. Brassat, and H. Bässler, "Charge carrier mobility in regioregular poly(3-hexylthiophene) probed by transient conductivity techniques: A comparative study," *Phys. Rev. B* **71**, 035214 (2005).
18. V. Kažukauskas, M. Pranaitis, V. Čyras, L. Sicot, and F. Kajzar, "Negative mobility dependence on electric field in poly(3-alkylthiophenes) evidenced by the charge extraction by linearly increasing voltage method," *Thin Solid Film* **516**, 8988–8992 (2008).
19. L. Xue, X. Gao, K. Zhao, J. Liu, X. Yu, and Y. Han, "The formation of different structures of poly(3-hexylthiophene) film on a patterned substrate by dip coating from aged solution," *Nanotechnology* **21**, 145303 (2010).
20. See, e.g., Table 1, G. Dennler, M. C. Scharber, and J. Brabec, "Polymer-fullerene bulk-heterojunction solar cells," *Adv. Mater.* **21**, 1–16 (2009).
21. E. Ehrenfreund, C. Lungenschmied, G. Dennler, H. Neugebauer, and N. S. Sariciftci, "Negative capacitance in organic semiconductor devices: Bipolar injection and charge recombination mechanism," *Appl. Phys. Lett.* **91**, 012112 (2007).
22. J. Bisquert, G. G. Belmonte, Á. Pitarch, and H. J. Bolink, "Negative capacitance caused by electron injection through interfacial states in organic light-emitting diodes," *Chem. Phys. Lett.* **422**, 184–191 (2006).

23. H. H. P. Gommans, M. Kemerink, and R. A. J. Janssen, "Negative capacitances in low-mobility solids," *Phys. Rev. B* **72**, 235204 (2005).
24. J. Huang, G. Li, and Y. Yang, "Influence of composition and heat-treatment on the charge transport properties of poly(3-hexylthiophene) and [6,6]-phenyl C_{61}-butyric acid methyl ester blends," *Appl. Phys. Lett.* **87**, 112105 (2005).

Biographies and photographs of the authors not available.